International Journal of Scientific Research in Science, Engineering and Technology

Print ISSN - 2395-1990
Online ISSN : 2394-4099

OPEN ACCESS

Available Online at : www.ijsrset.com
doi : https://doi.org/10.32628/IJSRSET2310524

Integrated Optimum Design of a Torsion Spring-Compensated Automotive Engine Hood Linkage Mechanism

Onur Denizhan*[1], Meng-Sang Chew[2]

*[1]Department of Electronics and Automation, Batman University, Batman, Türkiye

[2]Department of Mechanical Engineering and Mechanics, Lehigh University, Bethlehem, PA, USA

ARTICLEINFO

Article History :

Accepted: 07 Sep 2023
Published: 22 Sep 2023

Publication Issue :
Volume 10, Issue 5
September-October-2023

Page Number :
89-99

ABSTRACT

A torsion spring-assisted automotive hood linkage with joint friction is statically balanced for its entire range of motion. The four-bar linkage dimensions are to be synthesized. Coulomb friction at the joints can assist in the balancing. The magnitude of friction at the joints are unknown, and so are the torsion spring characteristics. All the aforementioned unknowns are determined in an integrated procedure such that the linkage dimensions, joint friction as well as the torsion spring are all designed optimally together in one go. The objective is to require the lowest force to close and to open the engine hood, with the entire design procedure to be performed in just one-step. Only three specifications are known: The mass characteristics (weight and center of gravity location) of the hood, the two acceptable regions of the hinge locations either on the engine hood or on the car body, as well as, the closed and opened positions of the engine hood. Thirty different design configurations (scenarios) are investigated and the results are discussed. The optimal results for a torsion spring-assisted hood linkage when compared to a similar tension spring-assisted linkage, show much better load compensation characteristics: The magnitudes and fluctuations of the external lifting force are smaller. Moreover, problem specification for a torsion spring system is also simpler.

Keywords: Four-Bar Mechanism, Kinematic Analysis, Optimization, Static Balancing, Springs

I. INTRODUCTION

The traditional design approach for the linkage mechanism is generally a two-step design procedure: First, synthesize a linkage mechanism for the application. Then, secondly, based on some desirable design objective, optimize the application based on the previously synthesized linkage. Note that in the second step, the synthesized linkage is no longer changeable; it is the application that is optimized relative to the fixed parameters of the already synthesized linkage.

The question is whether it is possible to optimize both the linkage and the application together so that the linkage as well as the application are optimally designed together. This article shows how this is done. Conceptually, such an approach should result in a better solution than one done in two steps. To be able to perform such a one-step integrated design process, one must be able to set up the design problem such that both the linkage synthesis procedure as well as its application must be combined into a single formulation. With such a formulation, changes in the linkage parameters can affect the application variables, and vice-versa. This article shows how such a formulation is carried out for a torsion spring-assisted hood linkage that results in a minimum external lifting-and-lowering force, in the presence of coulomb friction at the linkage joints.

II. PRIOR WORK

The following articles introduce traditional two or more steps in the design and optimization approaches of linkage systems. Yao et. al. [1] introduced a dual torsional spring-supported underactuated robotic finger mechanism analysis and optimal design. In this study, the robotic finger mechanism is designed. Then, based on some optimality criteria such as link lengths, link configurations and spring stiffness and damping, a multi-objective optimization is then applied at the second step. Quaglia and Yin [2], in their spring-supported planar articulated robots design for static balancing article, static balancing of their robot was also carried out in two steps. First, they performed a dynamic analysis of a given robot. In the second step, they then performed an optimization of the springs and links based on dynamic requirements of the articulated robot. A spring-supported statically balanced planar spring mechanisms computational design is presented by Takahashi et al. [3] wherein, the mechanism is defined in the first step, and then, a reduction and optimization of the mechanism is performed in the final step. Unfortunately, the solution through their multistep approach did not guarantee a statically balanced mechanism. A planar parallel cable-driven mechanism based on spring-loaded four-bar linkages for static balancing is investigated by Perreault et al. [4]. In the article, a nonlinear cable tension profile is first optimized, and then, the desired four-bar linkage input-output relationship is determined. The optimization perspective of this study is to have minimum cable tension subjected to a nonlinear spring-torque. In the optimum design of a parallel robot for medical 3D-Ultrasound imagining by Lessard et al. [5,6], three different static balancing approaches are introduced, such as, using a tension/compression spring, a torsion spring or a counterweight. After designing the mechanism in the first step, an input torque minimization is then carried out in the second step. In a study on static balancing of parallel robots by Russo et al. [7], a counterweight is used and the design process is also carried out in two steps. First, design the six-degree-of-freedom parallel robot and then, optimize the robot in the second step. Lamers et al. [8] designed a statically balanced fully compliant surgical grasper. In the first step, the latter is designed and then, optimized to improve behaviour of the design in the second step.

In a prior investigation, a one-step solution has been applied to the design of a tension-spring-assisted hood linkage [9,10]. In this present article, the one-step procedure is applied to the same system but using torsion-springs instead. Two cases resulting in a total of thirty different scenarios are investigated and the results will be presented and discussed.

III. PROBLEM DESCRIPTION

The primary aim of this study is to show the procedure to synthesize an optimum torsion spring-assisted automotive engine hood four-bar linkage mechanism for static balancing, in the presence of joint friction, and perform that procedure in one-step. What follows

is the process of formulating the problem so that it is amenable to the synthesis of the linkage as well as the optimization of the application, so that both are designed together.

A torsion spring-assisted four-bar linkage mechanism for the automotive engine hood is shown in Figs. 1a and 1b. All of the joints, the torsion springs, and rigid links are assumed massless. The following specifications of the automotive hood are known: Hood weight ($W = 11.68N$), hood length ($l_h = 1.2m$) and fully-closed and fully-opened positions of the engine hood are the only specifications needed for the procedure.

Two different cases are investigated: Case 1, shown in Fig. 2, refers to the design specification that Joint C and Joint D attachment points are not known and are to be optimally located on the hood while Joint A and Joint E are fixed on the vehicle body. Figure 3 shows Case 2 wherein; Joint C and Joint D are fixed on the automotive engine hood while Joint A and Joint E are attachment points to be optimally located on the vehicle body. For both these cases, circular bounds are assumed for the boundaries so that Joint C and Joint D in Case 1, and Joint A and Joint E in Case 2, can be located anywhere inside of the circular bound.

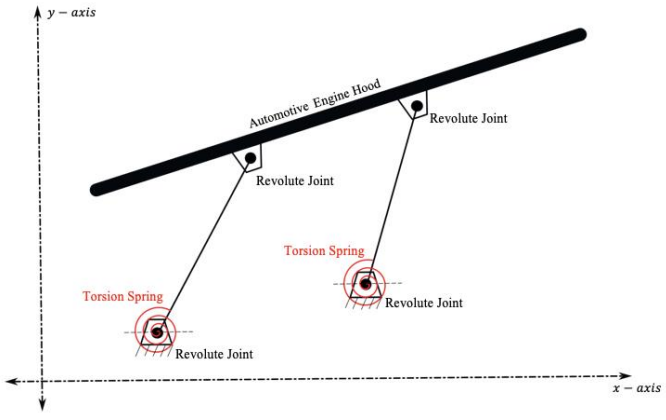

Figure 1a: The four-bar linkage mechanism for the engine hood with the two torsion springs

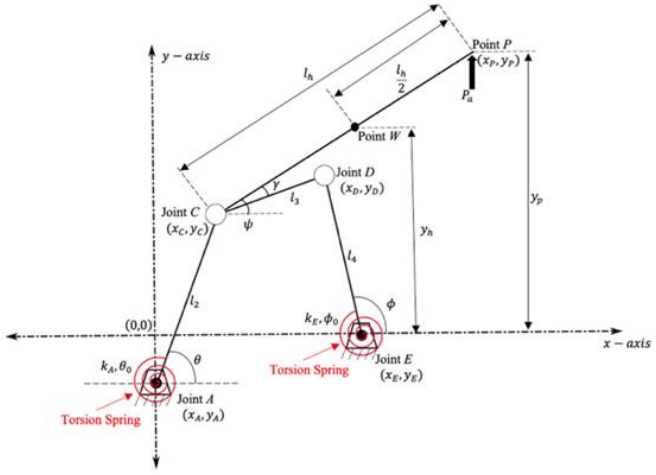

Figure 2b: The parameters of the four-bar linkage mechanism for the engine hood

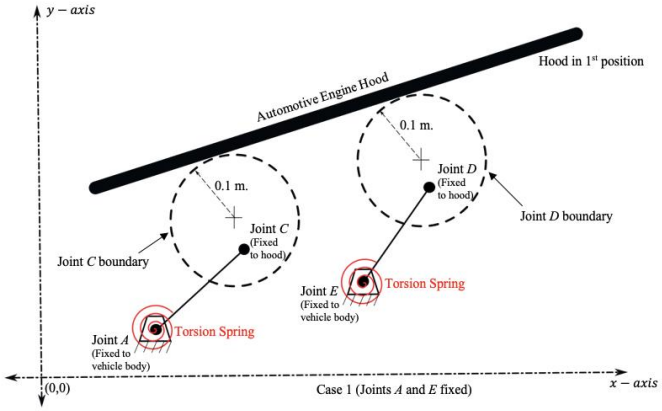

Figure 2: The Case 1: Joint A and Joint E fixed on the vehicle body

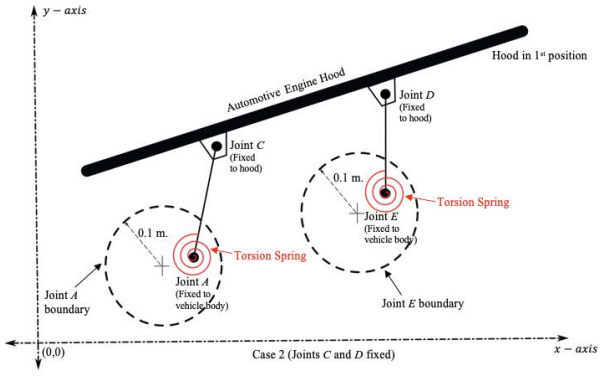

Figure 3: The Case 2: Joint C and Joint D fixed on the engine hood

Two torsion springs may be attached to the four-bar mechanism at the ground joints. The torsion springs can be either different or identical. In addition, different joint torque specifications can also be specified at the various linkage joints, resulting in five different scenarios for each case. These scenarios are:

- *Scenario 1*: Assumed only Joint *A* has the friction torque.
- *Scenario 2*: Assumed only Joint *C* has the friction torque.
- *Scenario 3*: Assumed only Joint *D* has the friction torque.
- *Scenario 4*: Assumed only Joint *E* has the friction torque.
- *Scenario 5*: Assumed all of the joints (Joints *A, C, D* and *E*) have the friction torque equally.

Figure 4 shows the cases and their related scenarios. As seen in Fig. 4, thirty different scenarios are investigated in this study totally.

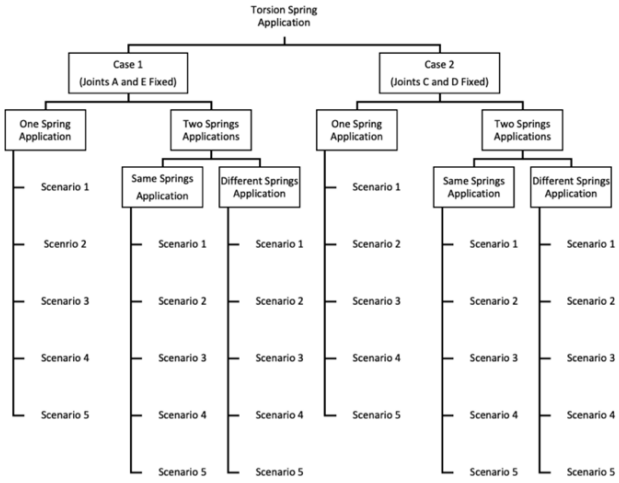

Figure 4: The torsion spring and joint friction scenarios

The same four-bar linkage mechanism for the automotive engine hood has been previously investigated and presented in [9,10]. The only difference is that torsion springs are incorporated at the ground joints instead of having a tension spring driving the drive link $[AC]$. All formulations are shown here in this article to illustrate the setup of the optimization problem.

A. Two-Position Kinematic Synthesis

A derivation of the equations for two-position kinematic synthesis of a four-bar linkage is first needed. All of the labels, vectors, and left and right-side dyads for two-position kinematic synthesis of the mechanism is shown in Fig. 5 below.

In Fig. 5, the four-bar is indicated by the four Joints *A, C, D* and *E*. Point *P* is a coupler point fixed on the link $[CD]$ so that the vectors $\overrightarrow{Z_1}$ and $\overrightarrow{Z_2}$ actually have the same length, and so is the lengths $|\overrightarrow{Z_1}|=|\overrightarrow{Z_2}|$.

Based on the Fig. 5, $[ED]$ and $[AC]$ dyads can be written as:

For the left-side dyad:

$$we^{i\theta_0} = \frac{ze^{i(\psi+\alpha)} - p_{12}e^{i\delta} - ze^{i\psi}}{1 - e^{i\theta_1}} \qquad (1)$$

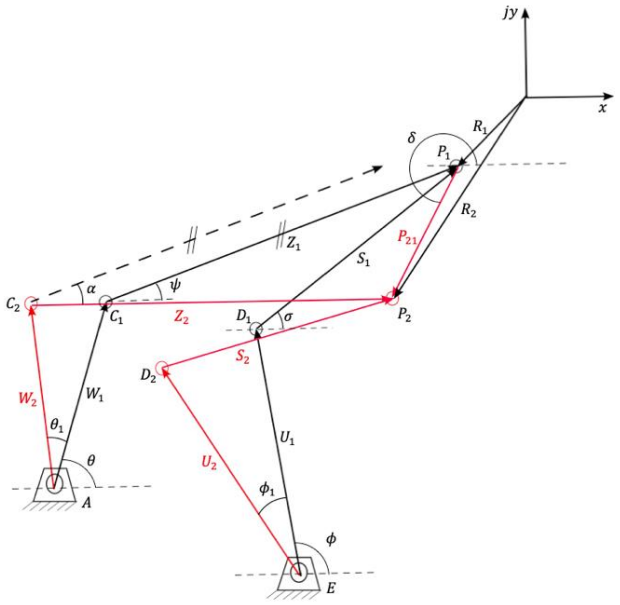

Figure 5: Two-position left and right-side dyads

For the right-side dyad:

$$ue^{i\phi_0} = \frac{se^{i(\sigma+\alpha)} - p_{12}e^{i\delta} - se^{i\sigma}}{1 - e^{i\phi_1}} \qquad (2)$$

where parameter θ_0 refers to the angle of $\overrightarrow{W_1}$ (link $[AC_1]$); θ_1, the angular difference between link $[AC_1]$ and link $[AC_2]$; σ, the angle of $\overrightarrow{S_1}$(link $[D_1P_1]$, first

position of link [DP]); α, the angular differences between two positions of link [CP]; ψ, angle of $\overrightarrow{Z_1}$ (link [C_1P_1]); ϕ_0, the angle of $\overrightarrow{U_1}$ (link [ED_1]); ϕ_1, the angular difference between two positions of link [ED]; δ, angle of $\overrightarrow{P_{12}}$ respectively. Parameter s refers to the length of the $\overrightarrow{S_1}$ and $\overrightarrow{S_2}$ ($|\overrightarrow{S_1}|=|\overrightarrow{S_2}|$, rigid link [$DP$]); z, the length of the $\overrightarrow{Z_1}$and $\overrightarrow{Z_2}$ ($|\overrightarrow{Z_1}|=|\overrightarrow{Z_2}|$, rigid link [$CP$]); u, the length of the $\overrightarrow{U_1}$ and $\overrightarrow{U_2}$ ($|\overrightarrow{U_1}|=|\overrightarrow{U_2}|$, rigid link [$ED$]); p_{12}, the length of the $\overrightarrow{P_{12}}$ ($|\overrightarrow{R_1}|$) respectively. In the two-position kinematic synthesis, there is a total of six free-choices [15] and these are assigned as design variables in the optimization procedure.

B. Virtual Work

For static balancing, the virtual work formulation requires that the latter vanishes. The two torsion springs-assisted four-bar engine hood mechanism is shown in Fig. 1b. The angle γ (angle between the links [CD] and [CP]) is constant and specified as 0.279 radian (16°) as shown in Fig. 1b. There are some differences between the tension spring-assisted and the torsion spring-assisted four-bar engine hood linkage mechanism: First, while tension spring-assisted hood mechanism requires spring attachment points on automotive body and link, the torsion spring-assisted hood mechanism does not require additional attachment points either on automotive body or link because the spring is attached at the joints. Secondly, the potential energy for torsion and tension springs are different from each other.

In this torsion spring-assisted four-bar engine hood linkage mechanism, coulomb friction is assumed in only four revolute joints (Joints *A, C, D* and *E*). When the hood is closed and opened, the coulomb friction at joints creates a resistance force to the engine hood motion and hence, it is crucial to correctly determine the direction of the joint friction torques. In the case of the hood opening, the links [ED] and [AC] move clock-wise, and the link [CD] moves counter-clock-wise directions. Friction at joints applies resisting torques to these links' motions; hence, the directions of the friction should be an inverse of the *relative* link rotations. Based on this knowledge, Joint A and Joint E friction directions should be in a counter-clockwise direction because of the links [AC] and [DE] have clockwise direction motions when the hood opens. On the other hand, Joint C and Joint D friction directions cannot be determined a priori based on hood and links motion directions because relative velocities are required to determine the friction directions in these joints. Previously, the kinematic analysis of the same mechanism motion was investigated and a clockwise friction direction at Joint C and a counter-clockwise friction direction at Joint D are found [9-13]. In this study, the counter-clockwise of friction direction is assumed as negative and the clockwise friction direction is assumed as a positive direction. In the same manner as the hood opening motion, the mechanism link motions and friction directions can be investigated. Following is the virtual work for the entire linkage:

$$\begin{aligned}\delta W = P_a \frac{\partial y_p}{\partial \theta} - \frac{\partial V_s}{\partial \theta} - \frac{\partial V_h}{\partial \theta} \pm T_A \\ \mp T_C\left(F_\psi - 1\right) \\ \pm T_D\left(F_\phi - F_\psi\right) \pm T_E F_\phi\end{aligned} \quad (3)$$

where δW refers to virtual work, P_a refers to applied force to engine hood, and ∂y_p refers to vertical virtual displacement of the point P (force applied point on the engine hood). Parameter ∂V_s is conservative potential of the torsion spring and parameter ∂V_h is conservative potential of automobile engine hood. Parameters T_A, T_C, T_D, and T_E are coulomb dry frictions at Joints *A, C, D,* and *E* respectively.

C. Optimization

The aim of optimization in this hood application is to minimize the magnitude of an externally applied force P_a to open or to close it. The quartic $\int (P_a)^4 d\theta$ form of objective function is chosen as the multi-objective function in this optimization setup. The reasons for this choice are given in [9].

The engine hood closing and opening forces are different in the presence of joint friction. Therefore,

there are two objective functions one for opening (P_{a_o}) and the other for closing (P_{a_c}) the hood. Based on the quartic multi-objective function form, a multi-objective as:

$$minimize: f = \eta_1 \int \left(P_{a_o}\right)^4 d\theta + \eta_2 \int \left(P_{a_c}\right)^4 d\theta \quad (4)$$

where η_1 and η_2 refer function weights in the optimization multi-objective function. P_{a_c} and P_{a_o} are the vertical forces to close and open the automobile hood respectively. Since the functions are quartic, they are always positive. The parameter θ is the angle of the engine hood relative to the horizontal axis and $\eta_1 = \eta_2 = 1$ so that the closing and opening forces are weighted equally.

The two-position kinematic synthesis has a total of six-free choices [14]. Four of these free choices (θ_1, ψ, σ and ϕ_1) can be set as design parameters in the optimization. The parameters z and s are other free-choices in the two-position synthesis formulation but they are assigned as initially known parameters in optimization and the parameter α in the two-position synthesis formulation can then be set as a design variable. The optimization in this study deals with linkage mechanism positioning based on a given linkage and hood dimensions; hence, parameters z and s are assigned as initially known parameters instead of optimization design variables. Because of two torsion springs, the optimization has 4 more design variables: Torsion spring constant and initial rotation angle in Joint A (k_A, θ_s) and torsion spring constant and initial rotation angle in Joint E (k_E, ϕ_s). With the unknown joint friction design parameters (T_A, T_C, T_D, and T_E), the multi-objective optimization has between 8 and 13 design variables based on the scenario.

Based on the mechanism practical usage and geometry of the torsion spring-assisted four-bar engine hood mechanism, boundaries for the design variables are specified. The details of these specifications are presented previously [9-10]. The optimization boundaries for the design variables are shown in Table 1.

The Joint A and Joint E are specified and are fixed locations on the car body in Case 1. The attachment coordinates for Joint $C(x_C, y_C)$ and Joint $D(x_D, y_D)$ on the engine hood are to be determined from the optimization process. In Case 2, Joints C and D are specified locations fixed on the hood while the attachment point coordinates (x_A, y_A), (x_E, y_E) of Joint A and Joint E respectively are assumed unknown but constrained to a circular bounded region on the vehicle body.

TABLE 1
BOUNDARY LIMITS FOR THE OPTIMIZATION FORMULATION

Design Variables	Lower Boundary	Upper Boundary
k_A(Nm/rad)	0.1	10^5
k_E(Nm/rad)	0.1	10^5
θ_1(rad)	0.3491	0.6981
θ_s (rad)	0	6.266
α (rad)	−1.309	−0.9599
ψ (rad)	0.7854	1.1345
ϕ_1 (rad)	0.4363	0.6109
ϕ_s (rad)	0	0.6266
σ (rad)	0.7854	1.1345
T_A (Nm)	0.1	10^5
T_C (Nm)	0.1	10^5
T_D (Nm)	0.1	10^5
T_E (Nm)	0.1	10^5

TABLE 2
OPTIMIZATION CONSTRAINTS FOR CASE 1 AND CASE 2

Case 1

minimize	$f = \eta_1 \int (P_{a_o})^4 d\theta + \eta_2 \int (P_{a_c})^4 d\theta$
subject to	$(x_C - x_{C_i})^2 + (y_C - y_{C_i})^2 < r^2$ $(x_D - x_{D_i})^2 + (y_D - y_{D_i})^2 < r^2$
Case 2	
minimize	$f = \eta_1 \int (P_{a_o})^4 d\theta + \eta_2 \int (P_{a_c})^4 d\theta$
subject to	$(x_A - x_{A_i})^2 + (y_A - y_{A_i})^2 < r^2$ $(x_E - x_{E_i})^2 + (y_E - y_{E_i})^2 < r^2$

The setup of the multi-objective problem with constraints (including Cases 1 and 2 boundary constraints) is summarized in Table 2 above. For Case 1, Joints C and D on the hood are unspecified, but are constrained to lie inside of some circular bounds. The coordinates (x_C, y_C), (x_D, y_D) refer to the respective centers of the circular bounds on the locations of Joints C and D while (x_{C_i}, y_{C_i}) and (x_{D_i}, y_{D_i}) refer to the actual coordinates of these joints that are constrained to be within the prescribed circular boundaries as set by the inequality constraints shown in Table 2. On the other hand, for Case 2, the ground joints A and E of the hood linkage are unspecified. Similarly, coordinates (x_A, y_A) and (x_E, y_E) refer to the respective centers of the circular bounds wherein the locations of Joints A and E can be located. The coordinates (x_{A_i}, y_{A_i}) and (x_{E_i}, y_{E_i}) refer to the actual coordinates of ground joints that are constrained to be inside of the respective circular boundaries.

For the boundaries of unknown joint locations in Cases 1 and 2, a perfect circle boundary is assumed to represent where each joint can be located. The radius of the perfect circle (r) boundary is set at $0.1m$ so that a circle centered at (m, n) with radius r is given by $(x - m)^2 + (y - n)^2 = r^2$ [15].

The formulation of the optimization problem is summarized in Table 2. This multi-objective optimization problem is then solved using a Sequential Quadratic Programming (SQP) algorithm [16].

IV. RESULTS

The results of this study present a total of thirty different scenarios; fifteen for each case. These are summarized in Tables 3, 4 and 5 along with Figs. 6 and 7. In each of these tables, results for Cases 1 and 2 are listed side-by-side, for ease of comparison. Table 3 shows the resulting linkage design with a single torsion spring attached at Joint A, while Table 4 shows the resulting design with two different optimized torsion springs at the ground Joints A and E. In contrast to Table 4, Table 5 shows the optimum results at the ground joints where torsion springs are constrained to be identical. All numerical results are rounded to three decimal place and N/A means the design variable is not part of the optimization in that Scenario. In these tables, S_1, S_2, S_3, S_4 and S_5 refer Scenarios 1 through 5 respectively. Figures 6 and 7 show the applied force to the hood for Scenario 3 in Cases 1 and 2 respectively. In the all these figures, the applied force to close and to open the hood in the presence of friction and without, are shown.

A. Case 1

Case 1 examines the situation when the Joint D and Joint C on the hood are unspecified but constrained to within a circular region for the optimization to determine. From Table 3, the lowest torsion spring constant required occurs in Scenario 2 (friction torque only at Joint C) while the highest spring constant occurs in Scenario 4 (with friction torque only at Joint E). However, the lowest friction torque required occurs in Scenario 5 (wherein all joints are applied the same friction torque) while the largest friction torque required occurs if it is only applied at Joint A (Scenario 1). The optimum results of the angles θ_1, ϕ_1, σ and ψ are the same in all five scenarios. Interestingly, the results in Table 3 show that the torsion spring does not require initial preload for Case 1.

Tables 4 and 5 show that the mechanism has either two identical or two different torsion springs, the spring constant has lower than a torsion spring assisted hood mechanism. Table 4 shows that the lowest spring

constant is required when Joint E has friction only (Scenario 4). Table 5 shows that the Scenario 2 gives the lowest torsion spring constant optimum result. Scenario 5 gives the lowest friction torque results in both Tables 4 and 5. This means that if friction torques are specified in all four joints, the torques required at each joint is minimum.

Figure 6 shows applied force for Case 1 in the presence of a single torsion spring with only joint friction at Joint D (Scenario 3). As seen in Fig 6, the required force to close and to open engine hood is always negative and positive, respectively. In the absence of joint friction, force applied is always positive (upward direction) to open and to close except at around the fully-open position. At the fully-open position a negative force (downward direction) is needed to keep the hood in equilibrium. This maximum required force value to close and to open the hood is between 5 and -5 N.

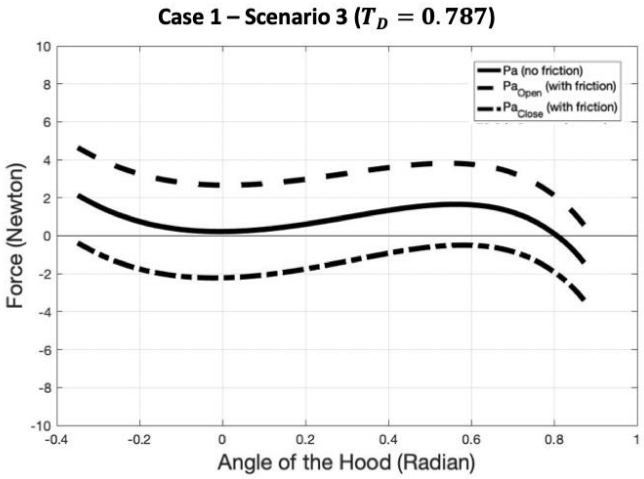

Figure 6: Applied force to hood with a single torsion spring-attached at Joint D

However, it should be noted that in the presence of joint friction, the hood will remain in equilibrium though its entire range of open positions. The dashed lines in this figure show the force needed to move the hood in one direction or other from its equilibrium condition.

B. **Case 2**

Case 2 examines the situation wherein the joints at the hood are specified, while those at the ground are constrained to within a circular region. The results when only a single torsion spring is attached are summarized in Table 3.

Table 3 shows that the lowest torsion spring constant result occurs in Scenario 3 wherein only Joint D has a friction torque of 0.847 Nm. No initial pre-load in the torsion spring is needed ($\theta_s = 0$), similar to Case 1 above. The lowest friction torque is required when all of the joints have the same friction (Scenario 5), again similar to Case 1. The optimum results for angles θ_1, ϕ_1, σ and ψ are the same across all five scenarios for both Cases 1 and 2.

Tables 4 and 5 summarize the situations when two torsion springs are applied at the ground joints: Joint A and Joint E. The torsion springs in the scenarios when both springs are identical, do not require an initial pre-load. Again, as in the single torsion spring design, the lowest friction torque occurs in Scenario 5 (friction is applied to all joints) and the same friction torque is applied within each scenario. Interestingly the same lowest friction torque is applied irrespective of whether two identical or two different torsion springs are used in the design. Furthermore, angles ϕ_1 and σ have the same optimum results across all scenarios in Case 2.

Figure 7 shows applied force for Case 2 in the presence of two torsion springs (identical and otherwise) with only joint friction at Joint D (Scenario 3). The required force value to close and to open the hood is between 4 and -4 N. Other scenarios for two-spring attached mechanisms have the similar results. Similar with Fig. 6, the engine hood requires upward direction force (positive) for opening and downward direction force (negative) for closing. However, it should be noted that if left at any given position in its range, the hood is statically balance.

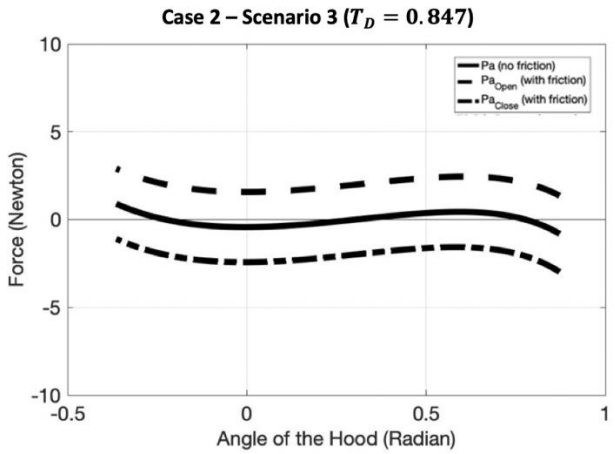

Figure 7: Applied force to hood with identical torsion springs-attached at Joint C and Joint D

The hood only requires upward and downward forces during the motion. On the other hand, in the absence of friction, a force is needed to keep the hood in equilibrium except for three metastable points.

TABLE 3
OPTIMUM RESULTS – SINGLE TORSION SPRING LINKAGE

Design Variables	CASE 1 (Joint A and Joint E Specified)					CASE 2 (Joint C and Joint D Specified)				
	S_1	S_2	S_3	S_4	S_5	S_1	S_2	S_3	S_4	S_5
k	54.633	45.101	49.541	58.809	53.244	32.441	31.433	32.123	34.844	32.239
θ_1	0.709	0.704	0.701	0.705	0.704	0.709	0.702	0.705	0.701	0.709
α	−1.204	−1.209	−1.201	−1.205	−1.204	−1.309	−1.302	−1.304	−1.305	−1.301
ψ	1.109	1.101	1.108	1.104	1.106	1.102	1.105	1.105	1.101	1.106
ϕ_1	0.406	0.405	0.401	0.403	0.404	0.409	0.408	0.404	0.401	0.409
σ	1.041	1.044	1.010	1.044	1.011	1.041	1.042	1.019	1.009	1.044
θ_s	0.001	0.009	0.044	0.011	0.005	0.032	0.002	0.004	0.002	0.050
T_A	1.939	N/A	N/A	N/A	0.244	1.444	N/A	N/A	N/A	0.240
T_C	N/A	0.544	N/A	N/A	0.238	N/A	0.725	N/A	N/A	0.229
T_D	N/A	N/A	0.787	N/A	0.239	N/A	N/A	0.644	N/A	0.212
T_E	N/A	N/A	N/A	1.811	0.209	N/A	N/A	N/A	0.914	0.239

TABLE 4
OPTIMUM RESULTS – DIFFERENT TORSION SPRINGS AT THE TWO GROUND JOINT A AND JOINT E

Design Variables	Different Springs at Joint A and Joint E									
	CASE 1 (Joint A and Joint E Specified)					CASE 2 (Joint C and Joint D Specified)				
	S_1	S_2	S_3	S_4	S_5	S_1	S_2	S_3	S_4	S_5
k_A	14.231	7.202	19.101	28.243	25.341	0.102	0.323	0.944	0.144	0.543
k_E	40.242	26.844	10.604	19.405	15.139	30.201	29.2	28.344	30.404	28.802
θ_1	0.705	0.704	0.609	0.609	0.601	0.709	0.703	0.706	0.705	0.702
α	−1.203	−1.209	−1.201	−1.208	−1.205	−1.203	−1.206	−1.201	−1.204	−1.205
ψ	1.101	1.023	1.039	1.044	1.012	1.102	1.003	1.100	1.102	1.104
ϕ_1	0.609	0.604	0.609	0.609	0.604	0.401	0.402	0.404	0.405	0.409
σ	1.029	0.903	0.903	0.908	0.905	1.039	1.001	1.041	1.009	1.029
θ_s	0.004	0.109	0.011	0.002	0.001	0.305	1.105	1.109	0.109	1.101
ϕ_s	0.104	0.104	0.109	0.020	0.009	1.107	1.109	1.108	1.108	1.105
T_A	1.240	N/A	N/A	N/A	0.144	2.444	N/A	N/A	N/A	0.343
T_C	N/A	0.641	N/A	N/A	0.139	N/A	1.101	N/A	N/A	0.341
T_D	N/A	N/A	0.134	N/A	0.124	N/A	N/A	0.847	N/A	0.339
T_E	N/A	N/A	N/A	0.222	0.108	N/A	N/A	N/A	1.644	0.301

TABLE 5
OPTIMUM RESULTS – IDENTICAL TORSION SPRINGS AT THE TWO GROUND JOINT A AND JOINT E

Design Variables	Identical Springs at Joint A and Joint E									
	CASE 1 (Joint A and Joint E Specified)					CASE 2 (Joint C and Joint D Specified)				
	S_1	S_2	S_3	S_4	S_5	S_1	S_2	S_3	S_4	S_5
k_A	13.844	8.641	9.141	7.722	10.244	21.932	21.403	21.202	22.609	21.804
k_E	13.844	8.641	9.141	7.722	10.244	21.932	21.403	21.202	22.609	21.804
θ_1	0.704	0.701	0.609	0.603	0.604	0.602	0.709	0.708	0.704	0.702
α	−1.201	−1.204	−1.202	−1.209	−1.204	−1.207	−1.201	−1.209	−1.204	−1.201
ψ	1.044	1.001	1.022	1.021	1.043	1.101	1.102	1.104	1.102	1.106

ϕ_1	0.601	0.609	0.603	0.604	0.605	0.403	0.402	0.404	0.405	0.394
σ	0.903	0.901	0.909	0.902	0.904	1.032	1.022	1.001	1.006	1.022
θ_s	0.003	0.011	0.010	0.020	0.033	0.002	0.006	0.010	0.031	0.005
ϕ_s	0.141	0.004	0.709	0.303	0.101	1.101	1.109	1.104	1.101	1.104
T_A	1.003	N/A	N/A	N/A	0.105	2.440	N/A	N/A	N/A	0.340
T_C	N/A	0.704	N/A	N/A	0.104	N/A	1.109	N/A	N/A	0.311
T_D	N/A	N/A	0.102	N/A	0.109	N/A	N/A	0.941	N/A	0.302
T_E	N/A	N/A	N/A	0.205	0.103	N/A	N/A	N/A	1.609	0.305

V. DISCUSSION

The results summarized in Figs. 6 and 7, show that the applied force fluctuation is minimal for closing and opening the automotive engine hood whether it is in the presence of joint friction or frictionless joints. In all of the scenarios, the hood is in a statically balanced position without any external force required, due to the presence of joint friction. Optimum designs results for single or double (identical or different) torsion springs across the different scenarios show only slight differences in the optimum parameters. This means that both of these designs can be chosen in whichever way that fits the practical application.

The optimum results of the design variables always tend to have values on bounds in given boundary conditions. Because of that, some optimum results of the angle θ_0 are vanishing. This means that the torsion springs in these scenarios are not pre-loaded.

This article investigated designs for the two-position synthesis of the hood linkage. However, this integrated one-step procedure is not limited to the four-bar linkage mechanism two-position kinematic synthesis. Increasing the number of positions will only reduce the number of design variables.

VI. CONCLUSION

In this study, a four-bar automotive engine hood linkage mechanism is synthesized, analysed and optimized in only one-step. The procedure integrates the four-bar-synthesis to the optimization of the rest of the parameters of all the other elements governing the static balance of the hood. Totally, thirty different scenarios are investigated and the optimum results are presented. The results show that the force curve fluctuation is small in the torsion spring-supported mechanism in the presence of joint friction. The torsion spring-assisted mechanism problem is simpler than that for the extension spring which requires additional parameters relating to the attachment locations of the tension spring. The force requirement to close or to open the automotive engine hood, with the torsion spring attached in the presence of joint friction, is low.

VII. REFERENCES

[1]. Yao, S., Ceccarelli, M., Carbone, G., Zhan, Q., & Lu, Z. (2011). Analysis and optimal design of an underactuated finger mechanism for LARM hand. Front. Mech. Eng.; 6:332. https://doi.org/10.1007/s11465-011-0229-8

[2]. Quaglia, G., Yin, Z., (2015). Static balancing of planar articulated robots. Front. Mech. Eng., 10:326–343. https://doi.org/10.1007/s11465-015-0355-9

[3]. Takahashi, T., Zehnder, J., Okuno, GH., Sugano, S., Coros, S., & Thomaszewski, B. (2019). Computational design of statically balanced planar spring mechanisms. in IEEE Robotics and Automation Letters Oct., 4(4):4438-4444. https://doi.org/0.1109/LRA.2019.2929984

[4]. Perreault, S., Cardou, P., & Gosselin, C. (2014). Approximate static balancing of a planar parallel

cable-driven mechanism based on four-bar linkages and springs. Mechanism and Machine Theory, 79:64-79. https://doi.org/10.1016/j.mechmachtheory.2014.04.008

[5]. Lessard, S., Bigras, P., Bonev, I., Briot, S., & Arakelian, V. (2007, Jun 17-21). Optimum static balancing of the parallel robot for medical 3D-ultrasound imaging. 12th IFToMM World Congress, Besançon, France. hal-00451939.

[6]. Lessard, S., Bigras, P., & Bonev, IA. (2007). A new medical parallel robot and its static balancing optimization. J. Med. Devices, 1(4):272-278. https://doi.org/10.1115/1.2815329

[7]. Russo, A., Sinatra, R., & Xi, F. (2005). Static balancing of parallel robots. Mechanism and Machine Theory, 40(2):191-202. https://doi.org/10.1016/j.mechmachtheory.2004.06.011

[8]. Lamers, AJ., Sanchez, JAG., & Herder, JL. (2015). Design of a statically balanced fully compliant grasper. Mechanism and Machine Theory, 92:230-239. https://doi.org/10.1016/j.mechmachtheory.2015.05.014

[9]. Denizhan, O., Chew, MS. (2023). Optimum synthesis and design of a hood linkage for static balancing in one-step. journal Tehnički vjesnik - Technical Gazette, 30(3): 855-862. https://doi.org/10.17559/TV-20221122144345

[10]. Denizhan, O. (2021). Incorporation of kinematic analysis, synthesis and optimization into static balancing (Publication No. 28716054) [Doctoral dissertation, Lehigh University]. ProQuest Dissertations & Theses Global.

[11]. Denizhan, O., Chew, MS. (2018). Linkage mechanism optimization and sensitivity analysis of an automotive engine hood. International Journal of Automotive Science and Technology, 2:7–16. https://doi.org/10.30939/ijastech..364438

[12]. Denizhan, O., Chew, MS. (2019). Optimum design of a spring-loaded linkage mechanism in the presence of friction for static balancing. Journal of Engineering Design and Analysis, 2(1):1–7. https://doi.org/10.24321/2582.5607.201901

[13]. Denizhan, O. (2015). Three-position four-bar linkage mechanism synthesis, static balancing and optimization of automotive engine hood (Publication No. 1599664) [Master's thesis, Lehigh University]. ProQuest Dissertations & Theses Global.

[14]. Norton, RL. (2019). Design of Machinery: An Introduction to the Synthesis and Analysis of Mechanisms and Machines (6th ed.). McGraw-Hill. ISBN-10: 1260113310.

[15]. Stillwell, J. (2010). The Four Pillars of Geometry, (1st ed.). Springer. ISBN-10: 1441920633.

[16]. Venkataraman, P. (2009). Applied Optimization with MATLAB Programming (2nd ed.). Wiley. ISBN: 978-0-470-08488-5.

Cite this article as :

Onur Denizhan, Meng-Sang Chew, " Integrated Optimum Design of a Torsion Spring-Compensated Automotive Engine Hood Linkage Mechanism , International Journal of Scientific Research in Science, Engineering and Technology(IJSRSET), Print ISSN : 2395-1990, Online ISSN : 2394-4099, Volume 10, Issue 5, pp.89-99, September-October-2023. Available at doi : https://doi.org/10.32628/IJSRSET2310524